Am J Physiol Cell Physiol 285: C102–C111, 2003;
10.1152/ajpcell.00583.2002.

Differential regulation of junctional complex assembly in renal epithelial cell lines

Shobha Gopalakrishnan, Mark A. Hallett, Simon J. Atkinson, and James. A. Marrs
Department of Medicine, Division of Nephrology, Indiana University Medical Center, Indianapolis, Indiana 46202-5181

Submitted 16 December 2002; accepted in final form 3 March 2003

Gopalakrishnan, Shobha, Mark A. Hallett, Simon J. Atkinson, and James. A. Marrs. Differential regulation of junctional complex assembly in renal epithelial cell lines. *Am J Physiol Cell Physiol* 285: C102–C111, 2003; 10.1152/ajpcell.00583.2002.—Several signaling pathways that regulate tight junction and adherens junction assembly are being characterized. Calpeptin activates stress fiber assembly in fibroblasts by inhibiting SH2-containing phosphatase-2 (SHP-2), thereby activating Rho-GTPase signaling. Here, we have examined the effects of calpeptin on stress fiber and junctional complex assembly in Madin-Darby canine kidney (MDCK) and LLC-PK epithelial cells. Calpeptin induced disassembly of stress fibers and inhibition of Rho GTPase activity in MDCK cells. Interestingly, calpeptin augmented stress fiber formation in LLC-PK epithelial cells. Calpeptin treatment of MDCK cells resulted in a displacement of zonula occludens-1 (ZO-1) and occludin from cell-cell junctions and a loss of phosphotyrosine on ZO-1 and ZO-2, without any detectable effect on tight junction permeability. Surprisingly, calpeptin increased paracellular permeability in LLC-PK cells even though it did not affect tight junction assembly. Calpeptin also modulated adherens junction assembly in MDCK cells but not in LLC-PK cells. Calpeptin treatment of MDCK cells induced redistribution of E-cadherin and β-catenin from intercellular junctions and reduced the association of p120ctn with the E-cadherin/catenin complex. Together, our studies demonstrate that calpeptin differentially regulates stress fiber and junctional complex assembly in MDCK and LLC-PK epithelial cells, indicating that these pathways may be regulated in a cell line-specific manner.

calpeptin; tight junctions; adherens junctions; Rho; cadherin; p120ctn

EPITHELIAL TRANSPORT FUNCTIONS are dynamically regulated in response to changing physiological conditions. Tight junction permeability is also dynamically regulated under various physiological conditions, and permeability varies along the length of the nephron. Different cell types within the nephron are produced during kidney development. These cells express different sets of genes that are reflected in different cell physiology and intracellular signaling mechanisms.

Epithelial junctional complexes include tight junctions and adherens junctions. Tight junctions, the apical-most junctional complex in epithelial cells, play a crucial role in maintaining epithelial cell polarity and regulating paracellular movement of solutes and ions across the epithelium (5, 8, 12, 24). Integral membrane proteins of the tight junction, occludin and claudin, are linked to the underlying actin cytoskeleton via their interaction with zonula occludens-1 (ZO-1) (36). Adherens junctions are adhesive structures formed by homotypic interactions between cadherin molecules on adjacent cells. The cytoplasmic domain of cadherins associates with β- or γ-catenin, and this complex is linked to the actin cytoskeleton by interaction with α-catenin (59).

Junctional complexes are also dysregulated by disrupted intracellular signaling pathways and as a pathophysiological consequence of disease (7, 36, 48). Disruption of the actin cytoskeleton and disassembly of junctional complexes play a major role in the pathophysiology of renal ischemia (37). Both the actin cytoskeleton and junctional complex assembly are regulated by members of the Rho GTPase family, and activation of the Rho signaling pathway protects tight junction assembly and the actin cytoskeleton during ATP depletion (an in vitro model for renal ischemia) (21, 43).

Rho GTPase (a member of the Ras superfamily of small GTP binding proteins) cycles between an active, GTP-bound conformation and an inactive, GDP-bound conformation, thereby regulating cell behavior and proliferation. Rho activation state is regulated by guanine nucleotide exchange factors (GEF), GTPase activating proteins (GAP), and guanine nucleotide dissociation inhibitors (GDI) (27). Rho GTPase regulates the formation of actin stress fibers and focal adhesions in various cell types (46). In epithelial cells, Rho signaling regulates tight junction assembly and function (21, 26, 40). Rho GTPase activity also controls establishment of cadherin-dependent cell-cell contacts in epithelial cells (11, 17, 20, 53).

Signaling pathways that activate Rho GTPase have not been completely characterized. Recently, the calpain inhibitor calpeptin was shown to activate Rho GTPase in fibroblasts by targeting the protein tyrosine phosphatase (PTPase) SH2-containing phosphatase-2 (SHP-2), which is an upstream inhibitor of Rho GTPase

Address for reprint requests and other correspondence: J. A. Marrs, Dept. of Medicine, Div. of Nephrology, Indiana Univ. Medical Center, R2 223, 950 West Walnut St., Indianapolis, IN 46202-5181 (E-mail: jmarrs@iupui.edu).

The costs of publication of this article were defrayed in part by the payment of page charges. The article must therefore be hereby marked "*advertisement*" in accordance with 18 U.S.C. Section 1734 solely to indicate this fact.

 0363-6143/03 $5.00 Copyright © 2003 the American Physiological Society

Downloaded from journals.physiology.org/journal/ajpcell (065.021.193.086) on March 14, 2022.

activity (49, 50). The effect of calpeptin on the Rho signaling pathway is independent of its effect on calpain. The SHP-2-Rho GTPase pathway was also previously shown to control hepatocyte growth factor-mediated cell scattering and to modulate the assembly/disassembly of stress fibers in Madin-Darby canine kidney (MDCK) cells (30). We have analyzed the effect of calpeptin in two epithelial cell lines, MDCK and LLC-PK cells. Calpeptin regulated stress fiber and junctional complex assembly differently in these two epithelial cell lines, indicating that cell type-specific differences exist in these pathway(s).

MATERIALS AND METHODS

Cells and reagents. MDCK type II cells were maintained in Dulbecco's modified Eagle's medium (DMEM; GIBCO BRL, Gaithersburg, MD) supplemented with 10% fetal bovine serum with penicillin, streptomycin, and glutamine (GIBCO Invitrogen, Grand Island, NY). LLC-PK porcine proximal tubule cells [American Type Culture Collection (ATCC), Manassas, VA] were maintained in 1:1 DMEM/F-12 (Sigma Chemical, St. Louis, MO) medium containing 10% fetal bovine serum, penicillin, and streptomycin. NIH-3T3 cells were maintained in DMEM supplemented with 10% fetal bovine serum, penicillin, and streptomycin.

Calpeptin and calpain inhibitor-1 (CI-1) were purchased from Calbiochem (San Diego, CA). Other chemicals were purchased from Sigma or Midwest Scientific (St. Louis, MO).

Rhodamine-phalloidin was purchased from Molecular Probes, (Eugene, OR). Antibodies against ZO-1 and occludin were from Zymed (San Francisco, CA). Monoclonal antibody 9E10 against the *myc* epitope was from Covance (Berkeley, CA). Monoclonal antibody (MAb) against RhoA was from Santa Cruz Biotechnology, (Santa Cruz, CA). The antibodies against p120ctn, E-cadherin, and horseradish peroxidase (HRP)-conjugated anti-phosphotyrosine antibody were purchased from BD Biosciences (San Diego, CA). The polyclonal antibodies against E-cadherin and β-catenin have been previously described (20, 35). MAb against E-cadherin (rr-1) was purchased from the Developmental Studies Hybridoma bank (maintained by the Department of Biological Sciences, University of Iowa, Iowa City, IA, under contract from National Institute of Child Health and Human Development).

Inhibitor treatment. NIH-3T3, MDCK, or LLC-PK cells were plated at a density of 2.0×10^5 per 35-mm culture dish. At 72 h postplating, cells were treated with CI-1 (10 μM) or calpeptin (100 μg/ml) diluted from DMSO stock solutions for 30 min at 37°C. DMSO (0.2% vol/vol) treatment was performed as a vehicle control for 30 min at 37°C. NIH-3T3 cells were serum-starved for 12 h before inhibitor treatment.

Transient transfection. MDCK or LLC-PK cells were plated at 2.5×10^5 per 35-mm culture dish. Cells were transfected 24 h later with 1.5 μg each of plasmids encoding RhoA-V14 or RhoA-N19 controlled by SV40 promoters (generously provided by Dr. Marc Symons, Picower Institute for Medical Research, Manhasset, NY) with Lipofectamine, according to manufacturer's protocol (Invitrogen, Carlsbad, CA). Cells were incubated with transfection mixture for 3–4 h. This mixture was then replaced with normal growth medium. Cells were analyzed at 30 h after transfection.

Preparation of GST Rho kinase binding domain. The pGEX vector encoding the Rho kinase Rho binding domain (ROK-BD, amino acids 941–1,075; a kind gift from Dr. Kaibuchi) (1) was transformed into *Escherichia coli* strain, BL21. Production of the fusion protein was initiated with isopropyl β-D-thiogalactopyranoside (IPTG). The fusion protein was isolated by binding to *S*-hexylglutathione-agarose. The glutathione *S*-transferase (GST)-bound fusion proteins bound to glutathione agarose (GST-ROK-BD) was stored aliquoted in liquid nitrogen for no more than 1 mo (9).

Rho GTPase pull-down assay. After cells were treated with inhibitors, they were rinsed once in phosphate-buffered saline (PBS) and lysed in *buffer A* [25 mM Tris·HCl, pH 7.5, 150 mM K acetate, 5 mM EDTA, 5 mM EGTA, 1 mM DTT, 10% glycerol, 1% TX-100, 60 mM OG (*n*-octyl β-D-glucopyranoside), and 1 mM PMSF, 1 mM benzamidine, 1 μg/ml pepstatin A, 40 μg/ml bestatin, 5 μg/ml leupeptin, 2 μg/ml aprotinin, and 100 μM butyrated hydroxy toluene] for 10 min on ice. Lysates were cleared by centrifugation for 5 s at 15,000 *g*. Lysate (25 μl) was then incubated with 30 μl of GST Rho kinase binding domain (GST ROK-BD) for 1 h at 4°C with rotation. Beads were washed three times in *buffer B* (25 mM Tris·HCl, pH 7.5, 150 mM K acetate, 5 mM EDTA, 5 mM EGTA, 1 mM DTT, and 10% glycerol). The unbound fractions from each wash were pooled, and TCA was precipitated. Beads were dried using a Speedvac (Savant Instruments, Holbrook, NY). Beads and TCA precipitates were resuspended in 50 μl of 2× SDS sample buffer (100 mM Tris·HCl, pH 6.8, 100 mM DTT, 2% SDS, 0.1% bromophenol blue, and 10% glycerol) and heated to 70°C for 5 min. Equal volumes from each fraction were analyzed on a 15% SDS polyacrylamide gel, transferred to Immobilon P^{SQ} (Millipore, Bedford, MA), and analyzed by Western blotting with an anti-RhoA antibody. Immunoblots were quantified using a Fluor-S MultiImager (Bio-Rad, Hercules, CA), and the results were presented as a ratio of active to inactive RhoA.

Paracellular permeability measurements. Cells were plated at a density of 2 million cells per filter on sixwell polycarbonate filter inserts (Corning-Costar, Kennebunk, ME) and grown for 6 days. Cells were washed in Ringer's buffer containing calcium (10 mM HEPES, pH 7.4, 154 mM NaCl, 7.2 mM KCl, and 1.8 mM $CaCl_2$). Ringer's buffer was added to the apical and basolateral compartments. Two μCi ^{3}H-inulin (Amersham Pharmacia, Piscataway, NJ) was added to the apical compartment, and filters were incubated at 4°C for 2 h. Fifty microliters of buffer were removed from the apical compartment, and 125 microliters buffer were removed from the basolateral compartment. Scintillation cocktail was added to these samples, and they were counted using a Beckman LS 5000 CE scintillation counter. Data were expressed as percent basolateral passage (basolateral counts/apical + basolateral counts × 100).

Immunofluorescence and image analysis. MDCK or LLC-PK cells plated on glass coverslips were fixed in PBS containing 4% paraformaldehyde for 10 min at room temperature. Cells were washed in PBS and then permeabilized in PBS containing 0.5% Triton X-100 for 5 min at room temperature. Cells were then blocked in PBS containing 0.2% BSA and 2% goat serum for 30 min at room temperature, followed by incubation with primary antibody diluted in block for 45 min at room temperature. Cells were washed in PBS containing 0.2% BSA and incubated with secondary antibodies diluted in block for 45 min at room temperature. Coverslips were washed and mounted in PBS containing 50% glycerol, 0.1% sodium azide, and 100 mg/ml 1,4-diazabicyclo[2.2.2]octane (DABCO).

For actin, cells were fixed in PBS containing 3.7% formaldehyde for 10 min at room temperature. After permeabilization and blocking (as described above), coverslips were incubated with 0.1 μg/ml rhodamine-phalloidin for 45 min at room temperature. Coverslips were then washed in PBS containing 0.2% BSA and mounted as described above.

Downloaded from journals.physiology.org/journal/ajpcell (065.021.193.086) on March 14, 2022.

Samples were viewed with a Bio-Rad MRC 1024 confocal microscope. Individual planes through the entire cell volume were collected at 0.5-μm intervals. Images representing stress fiber fluorescence were generated by summing five to six sections from the base of the cell that included all in-focus stress fiber fluorescence. For all other samples, a projection image was generated by summing the *z*-series images through the entire cell volume into one 16-bit image.

Immunoprecipitation. Inhibitor-treated cultures were rinsed in ice-cold PBS and lysed in CSK buffer [50 mM NaCl, 300 mM sucrose, 3 mM $MgCl_2$, 1 mM PMSF, 0.5% Triton X-100, and 10 mM PIPES, pH 6.8] for E-cadherin and β-catenin, in RIPA buffer (0.15 M NaCl, 1% Nonidet P-40, 0.5% deoxycholate, 0.1% SDS, 0.05 M Tris·HCl, pH 8.0) for ZO-1, and in NP-40-containing lysis buffer for p120ctn, for 15 min on ice. Monolayers were scraped and lysates were collected. Extracts were cleared by centrifugation at 15,000 *g* for 5 min at 4°C. Primary antibody was added to supernatants, and tubes were rotated at 4°C for 1 h. Immune complexes were collected with protein A-Sepharose beads (Amersham Pharmacia, Piscataway, NJ) or anti-mouse IgG-conjugated Sepharose beads (ICN Biomedical, Costa Mesa, CA) and washed three times in lysis buffers. Beads were resuspended in SDS-PAGE sample buffer and separated on 7.5% SDS polyacrylamide gels.

Immunoblotting. Samples separated by SDS-PAGE were transferred to nitrocellulose filters (Bio-Rad) and blocked in Tris-buffered saline containing Tween 20 (TBST; 10 mM Tris·HCl, pH 7.5, 100 mM NaCl, and 0.1% Tween 20) containing 3% BSA and 5% nonfat dry milk (for E-cadherin, β-catenin, and ZO-1), and in TBST containing 1% BSA for phosphotyrosine and p120ctn. Filters were incubated with primary antibody diluted in blocking solution for 1 h at room temperature. Filters were washed in TBST for 1 h. Filters were then incubated with species-matched, HRP-conjugated secondary antibody (Amersham Pharmacia) diluted in blocking solution. Filters were again washed in TBST, and signal was detected by enhanced chemiluminescence (ECL kit; Amersham Pharmacia) and exposed to film (Kodak Bio-Max ML; Eastman Kodak, Rochester, NY).

RESULTS

Calpeptin differentially regulates stress fiber assembly in MDCK and LLC-PK epithelial cells. Calpeptin, which inhibits SHP-2, a PTPase and activates Rho GTPase in fibroblasts (49, 50), was tested as an acute activator of Rho GTPase in epithelial cells. MDCK cells were treated with calpeptin or DMSO (vehicle control), and actin stress fibers were visualized by immunofluorescence using rhodamine-phalloidin. Calpeptin treatment resulted in disassembly of stress fibers in MDCK cells (Fig. 1), which was directly opposite of the expected effect if calpeptin activated Rho GTPase signaling. Interestingly, treatment of LLC-PK cells, another kidney epithelial cell line, with calpeptin induced stress fiber assembly (Fig. 1). The induction of stress fiber assembly in LLC-PK cells is similar to the previously reported effect of calpeptin on fibroblasts (49) (Fig. 1). Interestingly, the MDCK and LLC-PK cell lines displayed very different basal level of stress fibers, which may reflect differential regulation of the pathway leading to stress fiber assembly.

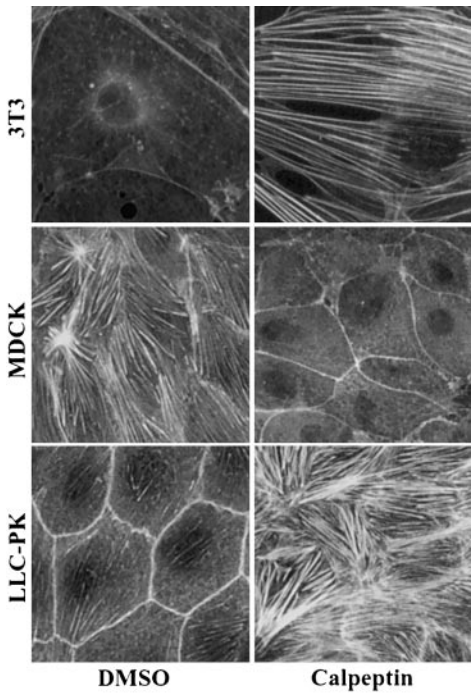

Fig. 1. Calpeptin differentially regulates stress fiber assembly in Madin-Darby canine kidney (MDCK) and LLC-PK cells. NIH-3T3, MDCK, or LLC-PK cells were plated on coverslips. At 3 days postplating, all 3 cell types were treated with calpeptin (0.1 mg/ml) or DMSO (vehicle control) for 30 min at 37°C, fixed, and stained for actin using rhodamine-phalloidin. Each image shown is 123.75 μm^2.

Calpeptin downregulates Rho GTPase activity in MDCK cells. To determine the effect of calpeptin treatment on Rho GTPase, its activity was measured using the pull-down assay (32). Cells lysates were incubated with GST-ROK BD (GST fusion protein containing the RhoA binding domain of Rho kinase) coupled to glutathione-Sepharose beads (1). Bound (active RhoA) and unbound (inactive RhoA) fractions were analyzed by SDS-PAGE, followed by Western blotting with an anti-RhoA antibody (Fig. 2, *C* and *D*). Rho GTPase activity was reduced in calpeptin-treated MDCK cells compared with the DMSO and CI-1 controls (Fig. 2*A*). CI-1 was used to control for any effects that could be due to calpain inhibition. A slight reduction in Rho activity was observed in CI-1-treated cells; however, this difference in Rho activity between DMSO and CI-1-treated cells was not statistically significant. We were unable to detect elevated Rho GTPase activity in LLC-PK cells that had been treated with calpeptin, despite dramatic induction of stress fiber assembly (Fig. 2*B*).

Calpeptin acts upstream from Rho GTPase in both MDCK and LLC-PK epithelial cells. To determine the placement of the calpeptin-sensitive activity within the Rho GTPase activation pathway, MDCK epithelial cells were transiently transfected with dominant active RhoA-V14, and cell cultures were treated with calpeptin at 30 h posttransfection. Cells were then double-labeled with rhodamine-phalloidin and anti-Myc antibodies to visualize stress fibers and Myc-epitope-

Downloaded from journals.physiology.org/journal/ajpcell (065.021.193.086) on March 14, 2022.

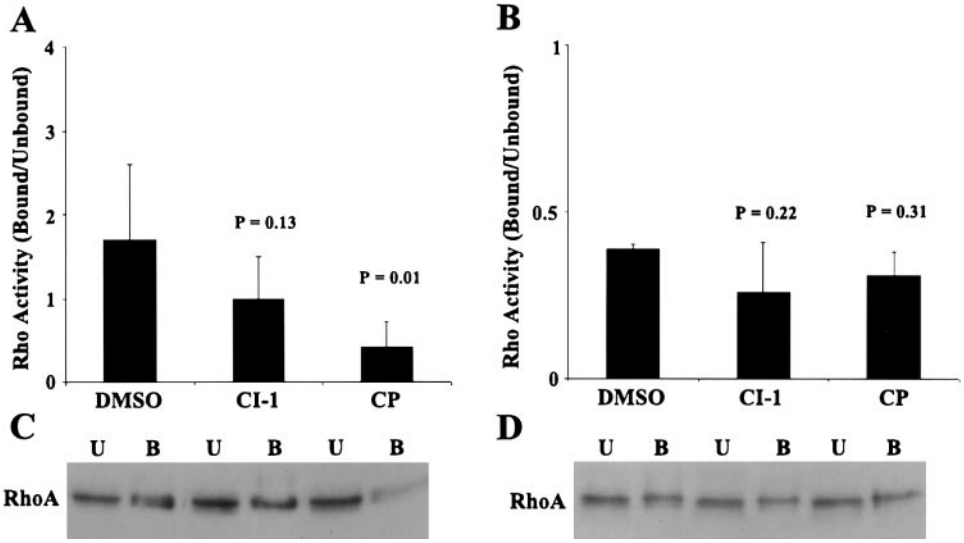

Fig. 2. Calpeptin inhibits Rho GTPase activity in MDCK cells. Confluent MDCK and LLC-PK cells were treated with DMSO, calpain inhibitor-1 (CI-1), or calpeptin for 30 min at 37°C. The levels of active Rho GTPase were analyzed by precipitating GTP-bound Rho GTPase with GST fusion protein containing the RhoA binding domain of Rho kinase (GST-ROK BD). Proteins bound to GST-ROK BD were analyzed by immunoblotting with an anti-RhoA antibody. Quantitation of immunoblots was performed using a Fluor-S MultiImager (Bio-Rad, Hercules, CA). The bars represent ratio of bound Rho to unbound Rho in each sample. *A*: Rho activity in MDCK cells decreased from 1.7 in DMSO-treated cells to 0.42 in calpeptin-treated cells ($P = 0.01$; *t*-test, $n = 10$). The difference in Rho activity between DMSO and CI-1-treated cells was not significant ($P = 0.13$). *B*: Rho activity in LLC-PK cells changed from 0.39 in DMSO-treated cells to 0.26 in CI-1-treated cells ($P = 0.22$; *t*-test, $n = 10$) and to 0.31 in calpeptin-treated cells ($P = 0.31$; *t*-test, $n = 10$). Data shown are representative of 5 independent experiments. Western blots of RhoA protein in the unbound (inactive) (U) and bound (active) (B) fractions from the Rho activity pull-down assay are shown in MDCK cells (*C*) and LLC-PK cells (*D*).

tagged RhoA-V14-expressing cells, respectively. In MDCK cells expressing the dominant active RhoA-V14 mutant, calpeptin treatment did not cause stress fiber disassembly (Fig. 3*A*). Rather, stress fibers remained abundant in these RhoA-V14-expressing cells, suggesting that calpeptin acts upstream of Rho GTPase in MDCK cells. LLC-PK cells transfected with dominant negative RhoA-N19 and treated with calpeptin at 30 h posttransfection were unable to support calpeptin-induced stress fiber assembly (Fig. 3*B*). However, a low level of stress fiber assembly could be detected in Rho-N19-expressing LLC-PK cells. This could be due to inability of Rho-N19 to sequester all of the exchange factors, thus leaving some activatable Rho that could respond to calpeptin. Alternatively, presence of stress fibers in Rho-N19 expressing LLC-PK cells treated with calpeptin suggests that calpeptin may also affect another signaling pathway in addition to Rho.

Calpeptin modulates tight junction assembly and function. Tight junction protein ZO-1 is serine/threonine and tyrosine phosphorylated (4, 52), and changes in ZO-1 phosphorylation have been implicated in tight junction assembly regulation (14, 57). Therefore, we analyzed the effect of calpeptin on ZO-1 phosphoryla-

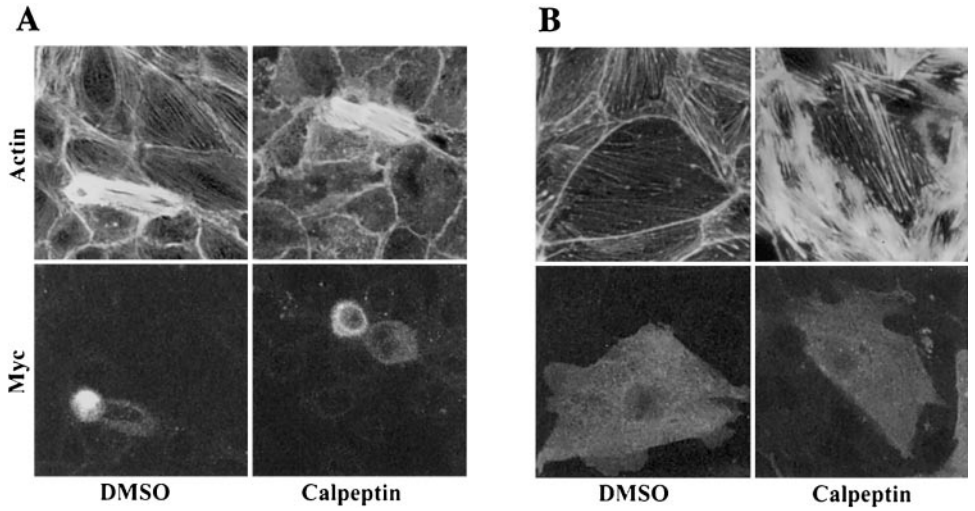

Fig. 3. Calpeptin acts upstream from Rho GTPase in both MDCK and LLC-PK cells. MDCK and LLC-PK cells were transiently transfected with Myc-tagged dominant active, RhoA-V14, or dominant-negative, RhoA-N19, respectively. At 30 h posttransfection, cells were treated with DMSO or calpeptin, fixed, and processed for double-label, indirect immunofluorescence using anti-Myc antibody to detect mutant Rho-expressing cells and rhodamine-phalloidin to detect actin stress fibers. *A*: MDCK cells expressing RhoA-V14 treated with DMSO or calpeptin and stained for actin stress fibers. *B*: LLC-PK cells expressing RhoA-N19 treated with DMSO or calpeptin and stained for actin stress fibers.

Downloaded from journals.physiology.org/journal/ajpcell (065.021.193.086) on March 14, 2022.

tion. Lysates from calpeptin- or control-treated MDCK cells were immunoprecipitated with anti-ZO-1 antibodies and probed for changes in phosphotyrosine content. ZO-2 coimmunoprecipitates in a complex with ZO-1, and both ZO-1 and ZO-2 are detected by antiphosphotyrosine antibodies in ZO-1 immunoprecipitates. Calpeptin caused a reduction of phosphotyrosine in ZO-1 and ZO-2 in MDCK cells (Fig. 4*A*).

Claudins comprise a family of transmembrane proteins that produce paracellular ion channels in various cell types (18, 19, 25). Different cell types express different combinations of claudin isoforms (56). Analysis of protein levels of claudins 1–4 in MDCK cells treated with calpeptin did not reveal any significant changes in calpeptin-treated cells compared with control cells (data not shown).

Subcellular distribution of tight junction proteins was examined in MDCK cells by indirect immunofluorescence. Calpeptin treatment reduced the amount of ZO-1 and occludin that was distributed at cell-cell junctions in MDCK cells (Fig. 4*C*). No change in claudin-1 distribution was observed in MDCK cells after calpeptin treatment (data not shown).

Treatment of LLC-PK cells with calpeptin did not change ZO-1 phosphorylation (Fig. 4*B*) or subcellular distribution of ZO-1 and occludin (Fig. 4*D*). As with MDCK cells, calpeptin treatment of LLC-PK cells did not affect claudin-1 protein levels or the subcellular distribution of claudin-1 (data not shown).

Paracellular permeability in calpeptin-treated MDCK and LLC-PK cells was assayed by using ^{3}H-inulin. No significant change in tight junction function was detected in MDCK cells (Fig. 5*A*). However, despite there being no change in tight junction protein phosphorylation or distribution, calpeptin increased inulin transport in LLC-PK cells from 3.2 ± 0.44 to 6.7 ± 0.94% basolateral passage ($P = 0.001$, $n = 6$) (Fig. 5*B*).

Calpeptin modulates adherens junction assembly. Adherens junction assembly is regulated by changes in phosphorylation of cadherin-associated catenins (15). The E-cadherin/catenin complex was immunoprecipitated from control- and calpeptin-treated MDCK or LLC-PK cells and probed for changes in phosphotyrosine content of the associated catenins by immunoblotting with antiphosphotyrosine antibodies. Calpeptin treatment of MDCK reduced the phosphotyrosine content in E-cadherin-associated β- and γ-catenins to 12 and 22% of control levels, respectively ($n = 3$) (Fig. 6*A*). The total cellular pool of β-catenin was also analyzed for changes in tyrosine phosphorylation after calpeptin treatment by immunoprecipitating β-catenin and immunoblotting these immunoprecipitates with antiphosphotyrosine antibodies. A nearly complete loss in phosphotyrosine content in β-catenin was observed after calpeptin treatment of MDCK cells (Fig. 6*C*). No change in phosphotyrosine content in cadherin-associated catenin was detected in LLC-PK cells after calpeptin treatment (Fig. 6*B*), but a slight increase in phosphotyrosine content of total cellular β-catenin was noted in LLC-PK cells that had been treated with CI-1 and calpeptin (Fig. 6*D*).

Subcellular distribution of E-cadherin, β-catenin, and p120ctn was examined by immunofluorescence. E-cadherin and β-catenin showed a slightly more diffuse distribution in calpeptin-treated MDCK cells relative to control cells (Fig. 6*C*); this effect was subtle but reproducible. However, p120ctn distribution in MDCK cells was not detectably changed after calpeptin treatment (Fig. 7*E*). Adherens junction protein distribution was not altered by calpeptin treatment in LLC-PK cells (Figs. 6*F* and 7*F*).

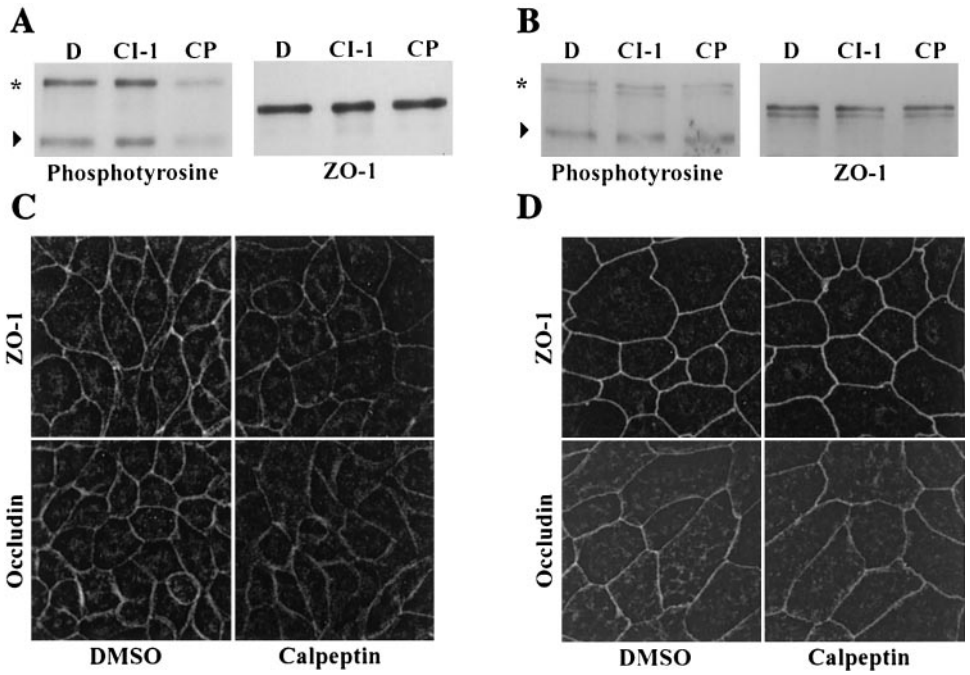

Fig. 4. Calpeptin regulates tight junction assembly in MDCK cells. MDCK or LLC-PK cells on glass coverslips or 35-mm dishes were treated with DMSO, CI-1, or calpeptin (CP) for 30 min at 37°C. Zonula occludens-1 (ZO-1) was immunoprecipitated from MDCK cells (*A*) or LLC-PK cells (*B*), separated by SDS-PAGE, transferred to nitrocellulose, and immunoblotted to detect phosphotyrosine (*left*) or ZO-1 (*right*). Asterisk denotes ZO-1 and arrowhead denotes ZO-2. MDCK cells (*C*) or LLC-PK cells (*D*) on coverslips were fixed and processed for indirect immunofluorescence using anti-ZO-1 or anti-occludin antibodies. Each image shown is 123.75 μm^2.

Downloaded from journals.physiology.org/journal/ajpcell (065.021.193.086) on March 14, 2022.

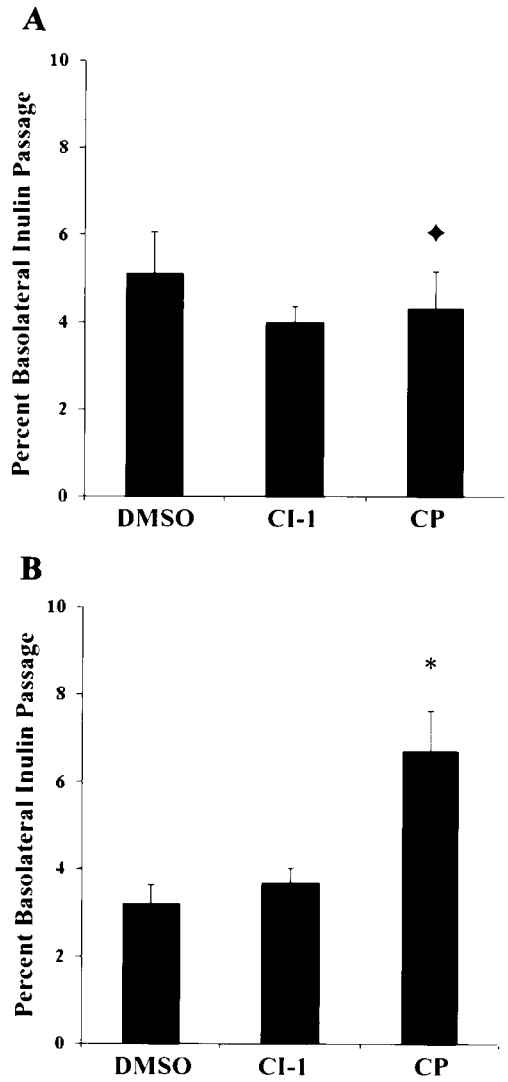

Fig. 5. Calpeptin regulates tight junction function in LLC-PK cells. MDCK and LLC-PK cells were cultured on permeable supports for 6 days and treated with DMSO, CI-1, or CP. Paracellular permeability was measured by ^{3}H-inulin passage from the apical to the basolateral compartment after 2 h at 4°C. Data are expressed as %basolateral passage (basolateral counts/apical + basolateral counts × 100). CP changed inulin transport in MDCK cells (*A*) from 5.1 ± 0.99 to 4.3 ± 0.86 (♦$P = 0.75$, *t*-test; $n = 6$) and increased inulin transport in LLC-PK cells (*B*) from 3.2 ± 0.44 to 6.7 ± 0.94% basolateral passage (*$P = 0.001$, *t*-test; $n = 6$).

The E-cadherin-associated protein p120ctn has been implicated in the modulation of cadherin adhesive activity (3), and tyrosine phosphorylation modulates p120ctn association with the E-cadherin/catenin complex (15). To study the effect of calpeptin on p120ctn phosphorylation, p120ctn was immunoprecipitated from control and calpeptin-treated cells and probed with antiphosphotyrosine antibody. Phosphotyrosine content was not detectable in p120ctn after calpeptin treatment of MDCK cells (Fig. 7*A*). In contrast, calpeptin did not alter p120ctn tyrosine phosphorylation in LLC-PK cells (Fig. 7*B*).

To examine the association of p120ctn with E-cadherin in response to calpeptin, p120ctn was immunoprecipitated from calpeptin-treated MDCK or LLC-PK cells, and the immunoprecipitates were immunoblotted to detect E-cadherin. The amount of E-cadherin that coimmunoprecipitated with p120ctn was reduced in calpeptin-treated MDCK cells (Fig. 7*C*), whereas the p120ctn/E-cadherin complex was not affected by calpeptin in LLC-PK cells (Fig. 7*D*).

Together, these results show that calpeptin inhibits Rho GTPase activity in MDCK epithelial cells and differentially regulates stress fiber and junctional complex assembly in MDCK and LLC-PK epithelial cells.

DISCUSSION

Calpeptin, a synthetic inhibitor of calpain, activates Rho GTPase in fibroblasts by inhibiting an upstream PTPase, SHP-2 (49, 50). In this study, we have shown that the calpeptin-sensitive pathway in MDCK epithelial cells is different from that in LLC-PK cells, showing that cell line-specific differences in calpeptin stimulation exist even among different renal epithelial cell lines. Interestingly, the induction of stress fiber assembly in LLC-PK cells was not accompanied by an increase in RhoA GTPase activity, suggesting the possibility that another signaling pathway may be regulated by calpeptin. It is also unclear whether other PTPases are affected by calpeptin in the epithelial cell lines that we tested, rather than SHP-2 that is inhibited in fibroblasts (50). However, we did determine that both MDCK and LLC-PK cells express equivalent amounts of SHP-2 (our unpublished observations).

Calpeptin treatment induced the loss of tight junction proteins ZO-1 and occludin from sites of cell-cell contact. We have previously shown that ZO-1 and occludin are displaced from cell-cell junctions in response to inhibition of Rho GTPase by dominant-negative Rho-N19 expression in MDCK cells (21). Similar observations have been made by other groups using C3 transferase to inhibit Rho GTPase in intestinal epithelial cells (40) and MDCK cells (53). In addition, phosphotyrosine content in ZO-1 and ZO-2 was reduced in response to calpeptin in MDCK cells. Several studies have suggested a role for tyrosine phosphorylation of ZO-1 in regulation of tight junction assembly (14, 55, 57). Surprisingly, the calpeptin-mediated disassembly of tight junctions was not accompanied by a change in tight junction function in MDCK cells, and calpeptin caused an increase in paracellular permeability of LLC-PK cells, even though it did not affect phosphorylation or assembly of ZO-1, occludin, or claudin. Increased paracellular permeability may be mediated via other, as yet unidentified tight junction proteins or indirectly through an effect on the actin cytoskeleton. Regulation of tight junction function in a cell line-specific manner is not unprecedented. The protein kinase C activator, phorbol 12-myristate 13-acetate, decreased tight junction conductance in LLC-PK monolayers but had the opposite effect in MDCK cells, indicating that regulatory pathways controlling tight junction function vary between different epithelial cell lines (16).

Downloaded from journals.physiology.org/journal/ajpcell (065.021.193.086) on March 14, 2022.

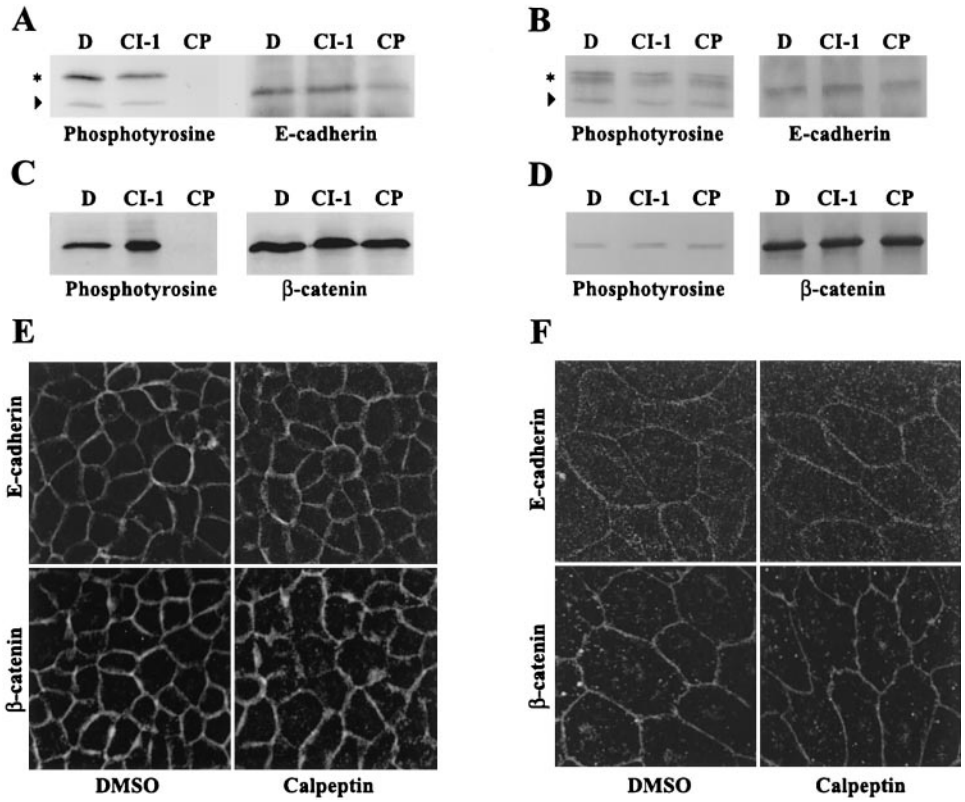

Fig. 6. Calpeptin regulates adherens junction assembly in MDCK cells. MDCK or LLC-PK cells on glass coverslips or 35-mm dishes were treated with DMSO, CI-1, or CP for 30 min at 37°C. MDCK (*A*) or LLC-PK cells (*B*) were extracted and immunoprecipitated with antibodies against E-cadherin, separated by SDS-PAGE, transferred to nitrocellulose, and probed with antibodies against phosphotyrosine (*left*) or E-cadherin (*right*). Asterisk denotes β-catenin and arrowhead denotes γ-catenin. MDCK (*C*) or LLC-PK cell (*D*) extracts were immunoprecipitated with anti-β-catenin antibodies and probed with antiphosphotyrosine (*left*) or β-catenin (*right*) antibodies. MDCK (*E*) or LLC-PK cells (*F*) on coverslips were fixed and processed for indirect immunofluorescence using anti-E-cadherin or anti-β-catenin antibodies. Each image shown is 123.75 μm^2.

In the kidney, different segments of the nephron exhibit varying tightness. The tight junctions in kidney proximal tubules are fairly leaky compared with the distal tubules (10). Furthermore, proximal tubules are more susceptible to ischemic injury than distal tubules (38, 58). Interestingly, LLC-PK cells are thought to be derived from proximal tubules and MDCK cells from distal tubules (23). However, it is not clear how closely these cell lines adhere to their original differentiated state, and properties characteristic of different tubule regions are coexpressed at the same time by these cells (12). Differential paracellular permeability along the nephron is governed, in part, by expression of specific combinations of claudins (29, 44). Paracellular permeability in epithelial cells is also regulated by various signaling pathways, and differential regulation of tight

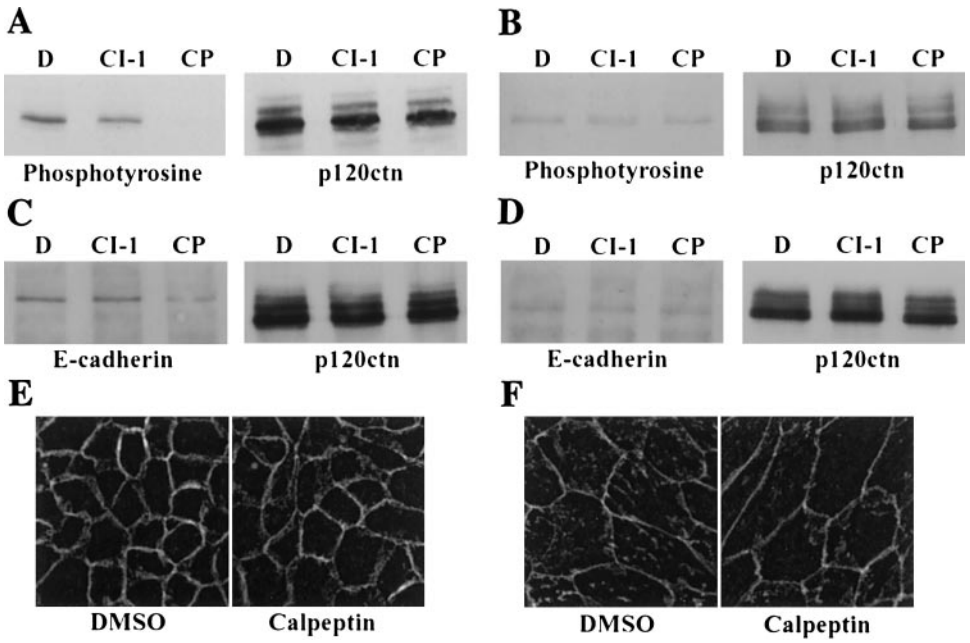

Fig. 7. Calpeptin regulates tyrosine phosphorylation and association of E-cadherin with p120ctn in MDCK cells. MDCK (*A*) or LLC-PK cells (*B*) treated with DMSO, CI-1, or calpeptin were extracted and immunoprecipitated with p120ctn antibodies, separated by SDS-PAGE, transferred to nitrocellulose, and probed with antibodies against phosphotyrosine (*left*) or p120ctn (*right*). MDCK (*C*) or LLC-PK cells (*D*) treated with DMSO, CI-1, or CP were extracted and immunoprecipitated with p120ctn antibodies, separated by SDS-PAGE, transferred to nitrocellulose, and probed with antibodies against E-cadherin (*left*) or p120ctn (*right*). MDCK (*E*) or LLC-PK cells (*F*) on coverslips were fixed and processed for indirect immunofluorescence using anti-p120ctn antibody. Each image shown is 123.75 μm^2.

Downloaded from journals.physiology.org/journal/ajpcell (065.021.193.086) on March 14, 2022.

junction function may thus reflect differences in regulatory pathways, such as the SHP-2 signaling pathway.

Calpeptin treatment of MDCK cells caused decreased distribution of E-cadherin and β-catenin at intercellular junctions, like that seen with inhibition of Rho GTPase by expression of dominant-negative Rho-N19 in MDCK cells (20) or C3 transferase in keratinocytes (11) and MDCK cells (53). Adherens junction assembly is regulated by tyrosine phosphorylation of catenins (15). Calpeptin-treated MDCK cells exhibited a loss of phosphotyrosine on β-, γ-, and p120ctn catenins. It is not clear how this change in catenin phosphorylation affects adherens junction assembly in calpeptin-treated MDCK cells.

Tyrosine phosphorylation of p120ctn regulates its association with cadherin: increased tyrosine phosphorylation of p120ctn may promote cadherin binding (3). In breast carcinoma cells, p120ctn exhibited stronger binding to E-cadherin when it was tyrosine phosphorylated (28). Similarly, phosphorylation of p120ctn by $pp60^{c\text{-}src}$ enhanced its ability to associate with E-cadherin by fourfold in in vitro experiments (47). Calpeptin treatment reduced p120ctn tyrosine phosphorylation and decreased its association with E-cadherin in coimmunoprecipitation experiments. Interestingly, cytosolic p120ctn has been reported to be unphosphorylated (41, 54), and free cytoplasmic p120ctn inhibits Rho GTPase activity (2, 22, 39), inducing a dendritic branching phenotype in cells (45). A role for tyrosine phosphorylation of p120ctn in Rho GTPase inhibition has not been established. However, the NH_2-terminal region of p120ctn that contains seven out of eight tyrosine phosphorylation sites (34) has been shown to be critical for induction of the dendritic branching phenotype. Reduced tyrosine phosphorylation of p120ctn induced by calpeptin may lead to an inhibition of Rho GTPase activity in MDCK cells by modulating the association of p120ctn with E-cadherin.

Alternatively, the loss of p120ctn tyrosine phosphorylation observed in calpeptin-treated MDCK cells may also be a consequence of Rho GTPase downregulation. In keratinocytes, Rho GTPases and *Fyn*/Src tyrosine kinases were implicated in positive regulation of cell-cell adhesion. Activated Rho GTPase was shown to increase tyrosine phosphorylation of p120ctn by activating PRK2, which activates *Fyn* tyrosine kinase (13). We have noted that expression of dominant-active Rho-V14 in MDCK cells caused an accumulation of p120ctn at sites of cell-cell contact, and expression of dominant-negative Rho-N19 caused a loss of p120ctn from cell-cell junctions (our unpublished observations).

Other potential regulation points of p120ctn on Rho signaling were examined during our studies. Association of p120ctn with vav2, a GEF for Rho family GTPases, regulates Rho GTPase activity (39). We were unable to detect any change in the p120ctn-vav2 complex in response to calpeptin treatment in MDCK cells (data not shown). Tyrosine phosphorylation of vav2 is another mechanism for regulating Rho GTPase activity (33, 51). We were unable to detect tyrosine phosphorylation of vav2 in control or calpeptin-treated MDCK cells (data not shown). Rho GTPase activity is also regulated by p190RhoGAP; tyrosine phosphorylated p190RhoGAP downregulates Rho GTPase activity (6). However, we did not detect an increase in tyrosine phosphorylation of p190RhoGAP in calpeptin-treated cells (data not shown).

SHP-2 plays an important role in several growth factor-mediated signaling pathways and has been demonstrated to bind several signaling intermediates (reviewed in Ref. 42). Recent studies in MDCK cells suggest an inhibitory effect of dominant active SHP-2 on Rho activity (31). This raises the possibility that calpeptin may regulate junctional complex assembly and function in MDCK and LLC-PK cells by targeting a protein other than SHP-2. Calpeptin induces stress fiber assembly in LLC-PK cells without an effect on Rho activity, suggesting that the calpeptin-sensitive signaling pathway may be completely separate from the Rho GTPase signaling pathway. The differential regulation of the actin cytoskeleton, cadherin/catenin complexes, and tight junctions by calpeptin in MDCK and LLC-PK cells also suggests that distinct regulatory pathways are functional in the two renal epithelial cell lines leading to differential regulation of cell adhesion and permeability.

We thank Dr. Marc Symons (Picower Institute for Medical Research, Manhasset, NY) for providing mutant RhoA expression plasmids. We also thank Dr. Bruce Molitoris for critical reading of the manuscript.

This work was supported by National Institute of Diabetes and Digestive and Kidney Diseases Grants DK-54518 and DK-53465 (to J. A. Marrs).

REFERENCES

1. **Amano M, Chihara K, Kimura K, Fukata Y, Nakamura N, Matsuura Y, and Kaibuchi K.** Formation of actin stress fibers and focal adhesions enhanced by Rho-kinase. *Science* 275: 1308–1311, 1997.
2. **Anastasiadis PZ, Moon SY, Thoreson MA, Mariner DJ, Crawford HC, Zheng Y, and Reynolds AB.** Inhibition of RhoA by p120 catenin. *Nat Cell Biol* 2: 637–644, 2000.
3. **Anastasiadis PZ and Reynolds AB.** The p120 catenin family: complex roles in adhesion, signaling and cancer. *J Cell Sci* 113: 1319–1334, 2000.
4. **Anderson JM, Stevenson BR, Jesaitis LA, Goodenough DA, and Mooseker MS.** Characterization of ZO-1, a protein component of the tight junction from mouse liver and Madin-Darby canine kidney cells. *J Cell Biol* 106: 1141–1149, 1988.
5. **Anderson JM and Van Itallie CM.** Tight junctions and the molecular basis for regulation of paracellular permeability. *Am J Physiol Gastrointest Liver Physiol* 269: G467–G475, 1995.
6. **Arthur WT, Petch LA, and Burridge K.** Integrin engagement suppresses RhoA activity via a c-Src-dependent mechanism. *Curr Biol* 10: 719–722, 2000.
7. **Balda MS, Gonzalez-Mariscal L, Contreras RG, Macias-Silva M, Torres-Marquez ME, Garcia-Sainz JA, and Cereijido M.** Assembly and sealing of tight junctions: possible participation of G-proteins, phospholipase C, protein kinase C and calmodulin. *J Membr Biol* 122: 193–202, 1991.
8. **Balda MS and Matter K.** Transmembrane proteins of tight junctions. *Semin Cell Dev Biol* 11: 281–289, 2000.
9. **Benard V, Bohl BP, and Bokoch GM.** Characterization of rac and cdc42 activation in chemoattractant-stimulated human neutrophils using a novel assay for active GTPases. *J Biol Chem* 274: 13198–13204, 1999.

Downloaded from journals.physiology.org/journal/ajpcell (065.021.193.086) on March 14, 2022.

10. **Boulpaep EL and Seely JF.** Electrophysiology of proximal and distal tubules in the autoperfused dog kidney. *Am J Physiol* 221: 1084–1096, 1971.
11. **Braga VM, Machesky LM, Hall A, and Hotchin NA.** The small GTPases Rho and Rac are required for the establishment of cadherin-dependent cell-cell contacts. *J Cell Biol* 137: 1421–1431, 1997.
12. **Brown D and Stow JL.** Protein trafficking and polarity in kidney epithelium: from cell biology to physiology. *Physiol Rev* 76: 245–297, 1996.
13. **Calautti E, Grossi M, Mammucari C, Aoyama Y, Pirro M, Ono Y, Li J, and Dotto GP.** Fyn tyrosine kinase is a downstream mediator of Rho/PRK2 function in keratinocyte cell-cell adhesion. *J Cell Biol* 156: 137–148, 2002.
14. **Chen Y, Lu Q, Schneeberger EE, and Goodenough DA.** Restoration of tight junction structure and barrier function by down-regulation of the mitogen-activated protein kinase pathway in *ras*-transformed Madin-Darby canine kidney cells. *Mol Biol Cell* 11: 849–862, 2000.
15. **Daniel JM and Reynolds AB.** Tyrosine phosphorylation and cadherin/catenin function. *Bioessays* 19: 883–891, 1997.
16. **Ellis B, Schneeberger EE, and Rabito CA.** Cellular variability in the development of tight junctions after activation of protein kinase C. *Am J Physiol Renal Fluid Electrolyte Physiol* 263: F293–F300, 1992.
17. **Fukata M and Kaibuchi K.** Rho-family GTPases in cadherin-mediated cell-cell adhesion. *Nat Rev Mol Cell Biol* 2: 887–897, 2001.
18. **Furuse M, Fujita K, Hiiragi T, Fujimoto K, and Tsukita S.** Claudin-1 and -2: novel integral membrane proteins localizing at tight junctions with no sequence similarity to occludin. *J Cell Biol* 141: 1539–1550, 1998.
19. **Furuse M, Furuse K, Sasaki H, and Tsukita S.** Conversion of zonulae occludentes from tight to leaky strand type by introducing claudin-2 into Madin-Darby canine kidney I cells. *J Cell Biol* 153: 263–272, 2001.
20. **Gopalakrishnan S, Dunn KW, and Marrs JA.** Rac1, but not RhoA, signaling protects epithelial adherens junction assembly during ATP depletion. *Am J Physiol Cell Physiol* 283: C261–C272, 2002.
21. **Gopalakrishnan S, Raman N, Atkinson SJ, and Marrs JA.** Rho GTPase signaling regulates tight junction assembly and protects tight junctions during ATP depletion. *Am J Physiol Cell Physiol* 275: C798–C809, 1998.
22. **Grosheva I, Shtutman M, Elbaum M, and Bershadsky AD.** p120 catenin affects cell motility via modulation of activity of Rho-family GTPases: a link between cell-cell contact formation and regulation of cell locomotion. *J Cell Sci* 114: 695–707, 2001.
23. **Gstrauthaler G, Pfaller W, and Kotanko P.** Biochemical characterization of renal epithelial cell cultures (LLC-PK1 and MDCK). *Am J Physiol Renal Fluid Electrolyte Physiol* 248: F536–F544, 1985.
24. **Gumbiner B.** Structure, biochemistry, and assembly of epithelial tight junctions. *Am J Physiol Cell Physiol* 253: C749–C758, 1987.
25. **Inai T, Kobayashi J, and Shibata Y.** Claudin-1 contributes to the epithelial barrier function in MDCK cells. *Eur J Cell Biol* 78: 849–855, 1999.
26. **Jou TS, Schneeberger EE, and Nelson WJ.** Structural and functional regulation of tight junctions by RhoA and Rac1 small GTPases. *J Cell Biol* 142: 101–115, 1998.
27. **Kaibuchi K, Kuroda S, and Amano M.** Regulation of the cytoskeleton and cell adhesion by the Rho family GTPases in mammalian cells. *Annu Rev Biochem* 68: 459–486, 1999.
28. **Kinch MS, Clark GJ, Der CJ, and Burridge K.** Tyrosine phosphorylation regulates the adhesions of *ras*-transformed breast epithelia. *J Cell Biol* 130: 461–471, 1995.
29. **Kiuchi-Saishin Y, Gotoh S, Furuse M, Takasuga A, Tano Y, and Tsukita S.** Differential expression patterns of claudins, tight junction membrane proteins, in mouse nephron segments. *J Am Soc Nephrol* 13: 875–886, 2002.
30. **Kodama A, Matozaki T, Fukuhara A, Kikyo M, Ichihashi M, and Takai Y.** Involvement of an SHP-2-Rho small G protein pathway in hepatocyte growth factor/scatter factor-induced cell scattering. *Mol Biol Cell* 11: 2565–2575, 2000.
31. **Kodama A, Matozaki T, Shinohara M, Fukuhara A, Tachibana K, Ichihashi M, Nakanishi H, and Takai Y.** Regulation of Ras and Rho small G proteins by SHP-2. *Genes Cells* 6: 869–876, 2001.
32. **Kranenburg O, Poland M, van Horck FP, Drechsel D, Hall A, and Moolenaar WH.** Activation of RhoA by lysophosphatidic acid and $G\alpha_{12/13}$ subunits in neuronal cells: induction of neurite retraction. *Mol Biol Cell* 10: 1851–1857, 1999.
33. **Liu BP and Burridge K.** Vav2 activates Rac1, Cdc42, and RhoA downstream from growth factor receptors but not β_1 integrins. *Mol Cell Biol* 20: 7160–7169, 2000.
34. **Mariner DJ, Anastasiadis P, Keilhack H, Bohmer FD, Wang J, and Reynolds AB.** Identification of Src phosphorylation sites in the catenin p120ctn. *J Biol Chem* 276: 28006–28013, 2001.
35. **Marrs JA, Napolitano EW, Murphy-Erdosh C, Mays RW, Reichardt LF, and Nelson WJ.** Distinguishing roles of the membrane-cytoskeleton and cadherin mediated cell-cell adhesion in generating different Na^+,K^+-ATPase distributions in polarized epithelia. *J Cell Biol* 123: 149–164, 1993.
36. **Mitic LL, Van Itallie CM, and Anderson JM.** Molecular physiology and pathophysiology of tight junctions. I. Tight junction structure and function: lessons from mutant animals and proteins. *Am J Physiol Gastrointest Liver Physiol* 279: G250–G254, 2000.
37. **Molitoris BA, Falk SA, and Dahl RH.** Ischemia-induced loss of epithelial polarity. Role of the tight junction. *J Clin Invest* 84: 1334–1339, 1989.
38. **Molitoris BA and Wagner MC.** Surface membrane polarity of proximal tubular cells: alterations as a basis for malfunction. *Kidney Int* 49: 1592–1597, 1996.
39. **Noren NK, Liu BP, Burridge K, and Kreft B.** p120 catenin regulates the actin cytoskeleton via Rho family GTPases. *J Cell Biol* 150: 567–580, 2000.
40. **Nusrat A, Giry M, Turner JR, Colgan SP, Parkos CA, Carnes D, Lemichez E, Boquet P, and Madara JL.** Rho protein regulates tight junctions and perijunctional actin organization in polarized epithelia. *Proc Natl Acad Sci USA* 92: 10629–10633, 1995.
41. **Ohkubo T and Ozawa M.** p120(ctn) binds to the membrane-proximal region of the E-cadherin cytoplasmic domain and is involved in modulation of adhesion activity. *J Biol Chem* 274: 21409–21415, 1999.
42. **Qu CK.** The SHP-2 tyrosine phosphatase: signaling mechanisms and biological functions. *Cell Res* 10: 279–288, 2000.
43. **Raman N and Atkinson SJ.** Rho controls actin cytoskeletal assembly in renal epithelial cells during ATP depletion and recovery. *Am J Physiol Cell Physiol* 276: C1312–C1324, 1999.
44. **Reyes JL, Lamas M, Martin D, Del Carmen Namorado M., Islas S., Luna J., Tauc M., and Gonzalez-Mariscal L.** The renal segmental distribution of claudins changes with development. *Kidney Int* 62: 476–487, 2002.
45. **Reynolds AB, Daniel JM, Mo YY, Wu J, and Zhang Z.** The novel catenin p120cas binds classical cadherins and induces an unusual morphological phenotype in NIH3T3 fibroblasts. *Exp Cell Res* 225: 328–337, 1996.
46. **Ridley AJ and Hall A.** The small GTP-binding protein Rho regulates the assembly of focal adhesions and actin stress fibers in response to growth factors. *Cell* 70: 389–399, 1992.
47. **Roura S, Miravet S, Piedra J, Garcia de Herreros A, and Dunach M.** Regulation of E-cadherin/catenin association by tyrosine phosphorylation. *J Biol Chem* 274: 36734–36740, 1999.
48. **Schneeberger EE and Lynch RD.** Structure, function, and regulation of cellular tight junctions. *Am J Physiol Lung Cell Mol Physiol* 262: L647–L661, 1992.
49. **Schoenwaelder SM and Burridge K.** Evidence for a calpeptin-sensitive protein-tyrosine phosphatase upstream of the small GTPase Rho. A novel role for the calpain inhibitor calpeptin in the inhibition of protein-tyrosine phosphatases. *J Biol Chem* 274: 14359–14367, 1999.

Downloaded from journals.physiology.org/journal/ajpcell (065.021.193.086) on March 14, 2022.

50. **Schoenwaelder SM, Petch LA, Williamson D, Shen R, Feng GS, and Burridge K.** The protein tyrosine phosphatase Shp-2 regulates RhoA activity. *Curr Biol* 10: 1523–1526, 2000.
51. **Schuebel KE, Movilla N, Rosa JL, and Bustelo XR.** Phosphorylation-dependent and constitutive activation of Rho proteins by wild-type and oncogenic *Vav*-2. *EMBO J* 17: 6608–6621, 1998.
52. **Staddon JM, Herrenknecht K, Smales C, and Rubin LL.** Evidence that tyrosine phosphorylation may increase tight junction permeability. *J Cell Sci* 108: 609–619, 1995.
53. **Takaishi K, Sasaki T, Kotani H, Nishioka H, and Takai Y.** Regulation of cell-cell adhesion by *rac* and *rho* small G proteins in MDCK cells. *J Cell Biol* 139: 1047–1059, 1997.
54. **Thoreson MA, Anastasiadis PZ, Daniel JM, Ireton RC, Wheelock MJ, Johnson KR, Hummingbird DK, and Reynolds AB.** Selective uncoupling of p120(ctn) from E-cadherin disrupts strong adhesion. *J Cell Biol* 148: 189–202, 2000.
55. **Tsukamoto T and Nigam SK.** Role of tyrosine phosphorylation in the reassembly of occludin and other tight junction proteins. *Am J Physiol Renal Physiol* 276: F737–F750, 1999.
56. **Tsukita S, Furuse M, and Itoh M.** Multifunctional strands in tight junctions. *Nat Rev Mol Cell Biol* 2: 285–293, 2001.
57. **Van Itallie CM, Balda MS, and Anderson JM.** Epidermal growth factor induces tyrosine phosphorylation and reorganization of the tight junction protein ZO-1 in A431 cells. *J Cell Sci* 108: 1735–1742, 1995.
58. **Weinberg JM.** The cell biology of ischemic renal injury. *Kidney Int* 39: 476–500, 1991.
59. **Yap AS, Brieher WM, and Gumbiner BM.** Molecular and functional analysis of cadherin-based adherens junctions. *Annu Rev Cell Dev Biol* 13: 119–146, 1997.

Downloaded from journals.physiology.org/journal/ajpcell (065.021.193.086) on March 14, 2022.